CHAPTER 18
FLYWHEELS

Daniel M. Curtis, Ph.D.
Senior Mechanical Engineer
NKF Engineering, Inc.
Reston, Virginia

LIST OF SYMBOLS

a	Constant, lb·s·ft/rad (J·s/rad)
A	Cross-sectional area of rim, in^2 (m^2)
A_s	Cross-sectional area of spoke, in^2 (m^2)
A_j, B_j, C_j	Difference coefficients
b	Constant, lb·ft (J)
C_s	Coefficient of speed fluctuation
C_u	Coefficient of energy fluctuation
D_j	Difference coefficient, lb (kN)
f_i	Intermediate variable
F	Stress function (= $rt\sigma_r$), lb (kN)
F_s	Geometric shape factor
g	Acceleration of gravity, 32.2 ft/s^2 (9.80 m/s^2)
I	Second moment of area, in^4 (m^4)
j	Index
J	Polar-mass moment of inertia, lb·s^2·ft (N·s^2·m)
K	Coefficient, 33 000 lb·ft·rpm/hp [2π J·rad/(W·s)]
n	Engine speed, rpm (rad/s)
N_c	Number of cylinders
N_s	Number of spokes
P	Power, hp (W)
r	Radial distance, in (m)

Δr	Radial-distance increment, in (m)
r_h	Hub radius, in (m)
r_a	Average radius of rim, in (m)
r_i	Inner radius of rim, in (m)
r_o	Outer radius of rim, in (m)
R	Specific energy, in (m)
S_y	Yield strength, psi (MPa)
t	Time, s
Δt	Time increment, s
T	Torque, lb·ft (J)
T_a	Angle-dependent torque, lb·ft (J)
T_s	Speed-dependent torque, lb·ft (J)
T_j	Torque at end of interval j, lb·ft (J)
U	Difference between the flywheel energy at maximum speed and at minimum speed, lb·ft (J)
V	Rim velocity, ft/s (m/s)
W	Weight, lb (kN)
z	Thickness, in (m)
z'	Radial derivative of flywheel thickness (= dz/dr)
z_0	Thickness at center, in (m)
Z_r	Section modulus of rim, in^3 (m^3)
Z_s	Section modulus of spoke, in^3 (m^3)
2α	Angle between adjacent spokes (see Fig. 18.6), rad
β	Angle, rad
θ	Angular position, rad
θ_{max}	Maximum angular deviation from constant-speed position, rad
θ_0	Angular position at start of machine cycle, rad
$\Delta\theta$	Angular increment, rad
ν	Poisson's ratio
ξ	Time, s
ρ	Weight density, lb/in^3 (kN/m^3)
σ	Stress, psi (MPa)
σ_0	Stress constant, psi (MPa)
σ_r	Radial stress, psi (MPa)
σ_t	Tangential stress, psi (MPa)
ω	Rotational speed, rad/s
ω_{max}, ω_{min}	Maximum and minimum speed, rad/s
ω_{avg}	Average speed [= $0.5(\omega_{max} + \omega_{min})$], rad/s
ω_0	Speed at start of machine cycle, rad/s
$\Delta\omega$	Maximum deviation of speed from average value, rad/s
ω_j	Speed at end of interval j, rad/s

The energy-storage capacity of a flywheel is determined from its polar moment of inertia J and its maximum safe running speed. The necessary inertia depends on the cyclic torque variation and the allowable speed variation or, in the case of energy-storage flywheels, the maximum energy requirements. The safe running speed depends on the geometry and material properties of the flywheel.

18.1 FLYWHEEL USAGE

Flywheels store energy. Indeed, flywheels are used as energy reservoirs, and this use will be discussed in Sec. 18.4. Their principal use in machine design, however, is to smooth the variations in shaft speed that are caused by loads or power sources that vary in a cyclic fashion. By using its stored kinetic energy $0.5J\omega^2$ to absorb the variations in torque during a machine cycle, a flywheel smooths the fluctuating speed of a machine and reduces undesirable transient loads. The effect of a flywheel is therefore fundamentally different from that of a regulator: A flywheel limits the speed variation over one cycle and has minimal effect on the average speed; a regulator uses negative feedback to maintain a selected average speed with only secondary effects on the speed during a cycle.

The flywheel has other features which have to be considered in design. Its size, speed, and windage effect can all be used to advantage in providing a secondary function as part of a clutch, gear, belt pulley, cooling fan, pump, gyroscope, or torsional damper.

18.2 SIZING THE FLYWHEEL

18.2.1 Coefficient of Speed Variation

A certain amount of fluctuation in shaft speed will not cause harmful torques or reduce the usefulness of a machine. The *coefficient of speed fluctuation* C_s is defined as

$$C_s = \frac{\omega_{max} - \omega_{min}}{\omega_{avg}} \tag{18.1}$$

where ω = rotational speed at the flywheel and ω_{avg} = average of ω_{max} and ω_{min}. Ranges for C_s for several categories of speed variation are given in Table 18.1. Assume that the system is stiff (the speeds of all shafts are proportional), that the external torque input or load is constant, and that ω_{avg} is close to the constant speed at which the energy from the average torque balances the external energy (this is usually a good assumption for values of C_s up to about 0.2). The energy equation $U = 0.5J(\omega_{max}^2 - \omega_{min}^2)$ and the definition of C_s combine to give the equation for the required mass moment of inertia [18.11]:

$$J = \frac{U}{\omega_{avg}^2 C_s} \tag{18.2}$$

This inertia includes the flywheel inertia and the inertia of all rotating parts, referred to the flywheel speed by multiplying by the square of the ratio of the shaft speeds (see Chap. 38).

TABLE 18.1 Suggested Values for the Coefficient of Speed Fluctuation C_s

Required speed uniformity	C_s
Very uniform	≤0.003
Moderately uniform	0.003–0.012
Some variation acceptable	0.012–0.05
Moderate variation	0.05–0.2
Large variation acceptable	≥0.2

Example 1. During each punching cycle, the cranking shaft for a punching operation does 270 J of work while rotating 30 degrees, as shown in Fig. 18.1. No work is done during the remaining 330 degrees. What size flywheel is necessary if the speed at the location of the flywheel is 20 rad/s and the inertia of the other rotating parts referred to the flywheel is 0.51 $N \cdot s^2 \cdot m$?

The average work required is $270/(2\pi) = 43.0$ J/rad. The motor will supply this constant torque throughout the cycle. Referring to Fig. 18.1, the flywheel will give up some of its stored energy during the 30 degrees of actual punching. This is the shaded area above the average-torque line; the motor will supply the additional 43 J/rad. During the remaining 330 degrees, the motor will resupply the flywheel, as shown by the shaded area below the average-torque line. The flywheel speed reaches its maximum and minimum where the loading torque crosses the average-torque line.

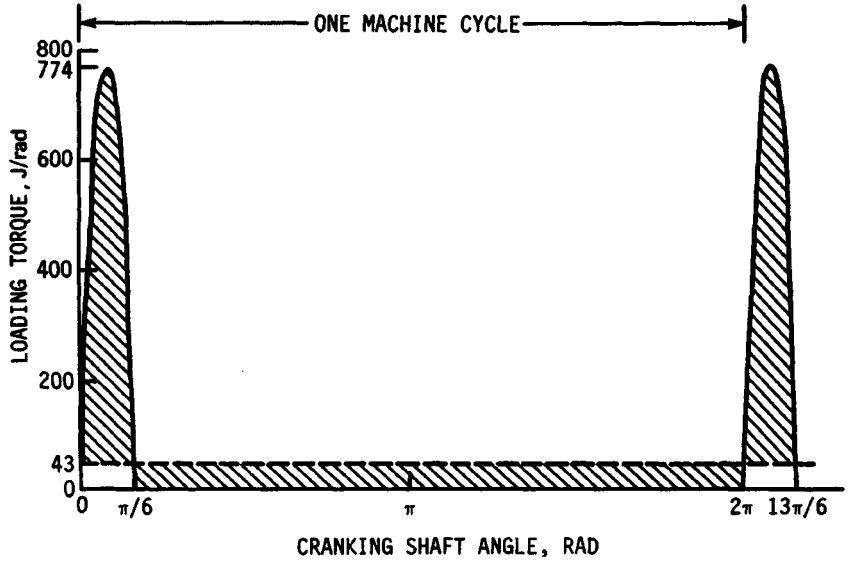

FIGURE 18.1 Torque-angle curve for punching operation in Example 1. The dashed line indicates the average torque of 43 J/rad, and the shaded areas are each equal to the maximum energy variation of 247 J.

Since the torque-angle curve is steep at both ends, the area above the average torque line is the total area minus the small rectangle below the average. The energy variation is then

$$U = 270 - 43.0\left(\frac{\pi}{6}\right) = 247 \text{ J} \tag{18.3}$$

The relative speed between the cranking shaft and the flywheel is unimportant since the energy (torque times angle) is the same at either speed. Letting $C_s = 0.10$ for a moderate speed variation, Eq. (18.2) gives the necessary flywheel inertia:

$$J = \frac{247}{20^2(0.10)} - 0.51 = 5.67 \text{ N}\cdot\text{s}^2\cdot\text{m} \tag{18.4}$$

For a steel-rim-type flywheel, assuming that 10 percent of the inertia is provided by the hub and spokes, the flywheel rim with a 0.5-m average rim diameter will weigh approximately

$$W = \frac{Jg}{r_a^2} = \frac{0.9(5.67)(9.80)}{0.25^2(1000)} = 0.800 \text{ kN} \tag{18.5}$$

Using a density of 76.5 kN/m^3, the necessary cross-sectional area is then given by

$$A = \frac{Jg}{2\pi\rho r_a^3} = \frac{0.9(5.67)(9.80)}{2\pi(76.5)(0.25)^3(1000)} = 0.006\,66 \text{ m}^2 \tag{18.6}$$

Assuming that the speed is at its average during the peak torque of 774 J, the peak power required without any flywheel effect would be

$$P = T\omega = 774(20)(0.001) = 15.5 \text{ kW} \tag{18.7}$$

Without a flywheel, the design limitation on the speed fluctuation would have to be met using a nonuniform input torque. With the flywheel, the required power is determined from the average torque of 43.0 J:

$$P = T\omega = 43.0(20)(0.001) = 0.9 \text{ kW} \tag{18.8}$$

This shows that in addition to smoothing the machine operation, the flywheel actually reduces the size of the motor required.

18.2.2 Integration of the Torque-Angle Relation

If the torque-angle curve for a machine cycle is available from experimental data or a dynamic analysis, U is determined from the areas between the curve and the average-torque line. If the external torque input or load is not constant, it can be combined with the torque-angle curve for the machine. If the loading torque and the driving torque are not synchronized or have an unknown phase difference, a worst-case combination should be used. The areas under the curve can be determined using a planimeter or by graphic or numerical integration as shown in Chap. 4. (See also Example 4 or consult the user handbook for your programmable calculator or computer.) Unless C_s is accurately known and the curve is from a worst case or is highly repeatable, precision in integrating is not warranted.

Example 2. An engine has the torque-angle curve given in Fig. 18.2. If the average speed at the flywheel is 2000 rpm and the output speed is allowed to vary by ±2.5 percent, how large a flywheel is necessary if the loading torque is assumed constant? The inertia of the other rotating parts, referred to the flywheel, is 0.11 lb·s²·ft.

The net area under the curve, using a planimeter, is 1156 lb·ft. One machine cycle for the four-stroke engine consists of two crankshaft cycles. The average torque is therefore $1156/(4\pi) = 92.0$ lb·ft. This average torque is shown as the dashed line in Fig. 18.2. The maximum and minimum velocities will occur at the points where the curve crosses this line. Each area between crossover points is measured and tabulated (see Table 18.2). The relative maxima and minima of the speed occur at the crossover points; therefore, the largest energy difference between any two crossover points will determine U. Since these two points will not necessarily be adjacent to each other, a running sum of the individual areas $A + I$ through H is formed, starting at an arbitrary crossover point. The largest energy difference is then the maximum sum minus the minimum sum; in this case, $U = 1106 - (-95) = 1201$ lb·ft. With $\omega = 2\pi(2000)/60 = 209.4$ rad/s and $C_s = 2(0.025) = 0.05$, Eq. (18.2) gives

$$J = \frac{1201}{209.4^2(0.05)} - 0.11 = 0.438 \text{ lb}\cdot\text{s}^2\cdot\text{ft} \tag{18.9}$$

Note that if the engine were operated at a slower speed, Eq. (18.2) indicates that a larger flywheel would be necessary even if the torque-angle curve did not change.

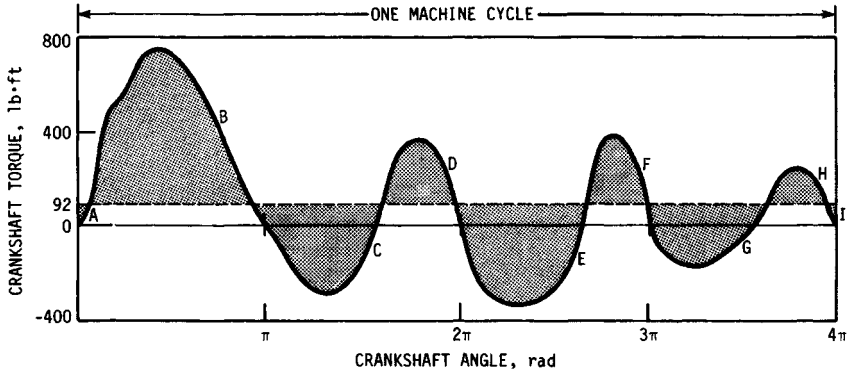

FIGURE 18.2 Torque-angle curve for the engine in Example 2. The dashed line indicates the average torque of 92.0 lb·ft, and the shaded areas are the energy variations from the average speed. Sections A and I correspond to the values given in Table 18.2.

TABLE 18.2 Area Sums for Example 2

Section	$A + I$	B	C	D	E	F	G	H
Area, lb·ft	−18	1124	−550	242	−710	208	−391	95
Sum, lb·ft	−18	1106	556	798	88	296	−95	0
Extreme values, lb·ft		1106					−95	

18.2.3 Coefficient of Energy Variation

The torque-angle relationship for an engine depends on the fuel, gas pressures, reciprocating masses, speed, and engine geometry [18.2]. The large variation that is possible between different engine designs shows that dynamic measurement or kinematic analysis is necessary to determine the torque fluctuation. It is often necessary, however, to come up with a rough estimate for preliminary design purposes or for checking the reasonableness of calculated values. For these purposes, the energy variation for an internal-combustion engine can be estimated by

$$U = C_u \frac{KP}{\omega} \tag{18.10}$$

where $K = 33\,000$ lb·ft·rpm/hp [2π J·rad/(W·s)]. The coefficient of energy variation C_u can be approximated for a two-stroke engine with from 1 to 8 cylinders using the equation

$$C_u = \frac{7.46}{(N_c + 1)^3} \tag{18.11}$$

and for a four-stroke engine with from 1 to 16 cylinders using the two-branched equation

$$C_u = \frac{0.8}{|N_c - 1.4|^{1.3}} - 0.015 \tag{18.12}$$

Example 3. A 150-hp four-cylinder, four-stroke engine has a flywheel speed of 1000 rpm. Estimate the flywheel necessary for a 2 percent speed variation with a uniform load at an engine speed of 3000 rpm, neglecting the flywheel effect of the other rotating parts.

Using Eq. (18.12),

$$C_u = \frac{0.8}{|4 - 1.4|^{1.3}} - 0.015 = 0.22 \tag{18.13}$$

Then from Eq. (18.10),

$$U = 0.22 \frac{33\,000(150)}{3000} = 363 \text{ lb·ft} \tag{18.14}$$

so that from Eq. (18.2), with $\omega = 2\pi(1000)/60 = 105$ rad/s,

$$J = \frac{363}{105^2(0.02)} = 1.6 \text{ lb·s}^2\text{·ft} \tag{18.15}$$

18.2.4 Angular Fluctuation

Certain machines, such as electric generators and magnetic digital storage systems, must maintain their angular position within a close tolerance of the constant-speed position. If the torque is known as a function of time, it can be integrated to deter-

mine the angular velocity, and then the angular velocity can be integrated to give the angular position:

$$\omega(t) = \int_0^t \frac{T(\xi)}{J}\, d\xi + \omega_0 \tag{18.16}$$

$$\theta(t) = \int_0^t \omega(\xi)\, d\xi + \omega_0 t + \theta_0 \tag{18.17}$$

where the $\omega_0 t + \theta_0$ term represents the constant-speed position.

In the more usual instance, the torque is known only as a function of angle. For small values of C_s, however, the torque-time curve is indistinguishable from the torque-angle curve with the angle coordinate divided by ω_{avg}.

Example 4. A generator with the input torque given in Fig. 18.3*a* must maintain an angular position within ±0.25 degrees of the uniform 200-rpm position. Assuming a uniform load, what flywheel inertia is necessary?

For illustration purposes, the machine cycle will be divided into 10 intervals of $\Delta t = 0.03$ s each, as shown in Fig. 18.3*a*. For an accurate solution, the problem would be programmed with perhaps 20 intervals.

The torque at each step is tabulated (column 3 in Table 18.3), and then the average torque in each interval is placed in column 4. This value, if multiplied by Δt, would be the area below the curve using the trapezoid rule. Adding these average torques (column 5) and dividing by 10 intervals gives the average torque for the curve, 902 lb·ft (column 6), shown as the dashed line in Fig. 18.3*a*. Subtracting this average, the constant loading torque, from column 4 gives column 7, the average excess of supplied torque in each interval. The running sum of these values (column 8) performs the integration, to give $J\omega/\Delta t$ (see Fig. 18.3*b*). The relative speed at the end of each interval is therefore the value in column 8 times $\Delta t/J$.

The procedure is repeated for the second integration, giving columns 9 through 13. Column 13 is then $J\theta/(\Delta t)^2$ (Fig. 18.3*c*), so that the relative angular position is the value in column 13 times $\Delta t^2/J$. The maximum range in column 13 is 6915 – (–7725) = 14 640 lb·ft. The maximum angular deviation from the mean position is calculated from half the maximum range, so that

$$\theta_{max} = \frac{(\Delta t)^2(14\,640)}{J(2)} \tag{18.18}$$

For $\theta_{max} = 0.25$ degrees = 0.004 36 rad deviation, this gives

$$J = \frac{0.03^2(14\,640)}{0.004\,36(2)} = 1511 \text{ lb}\cdot\text{s}^2\cdot\text{ft} \tag{18.19}$$

The speed variation is determined as a by-product of the process. The maximum range in column 8 is 9878 – 0 = 9878 lb·ft. The maximum speed variation is then

$$\omega_{max} - \omega_{min} = \frac{\Delta t(9878)}{J} = \frac{0.03(9878)}{1511} = 0.196 \text{ rad/s} \tag{18.20}$$

For $\omega_{avg} = 2\pi(200)/60 = 20.94$ rad/s, the coefficient of speed fluctuation is then, from Eq. (18.1),

$$C_s = \frac{0.196}{20.94} = 0.009\,36 \tag{18.21}$$

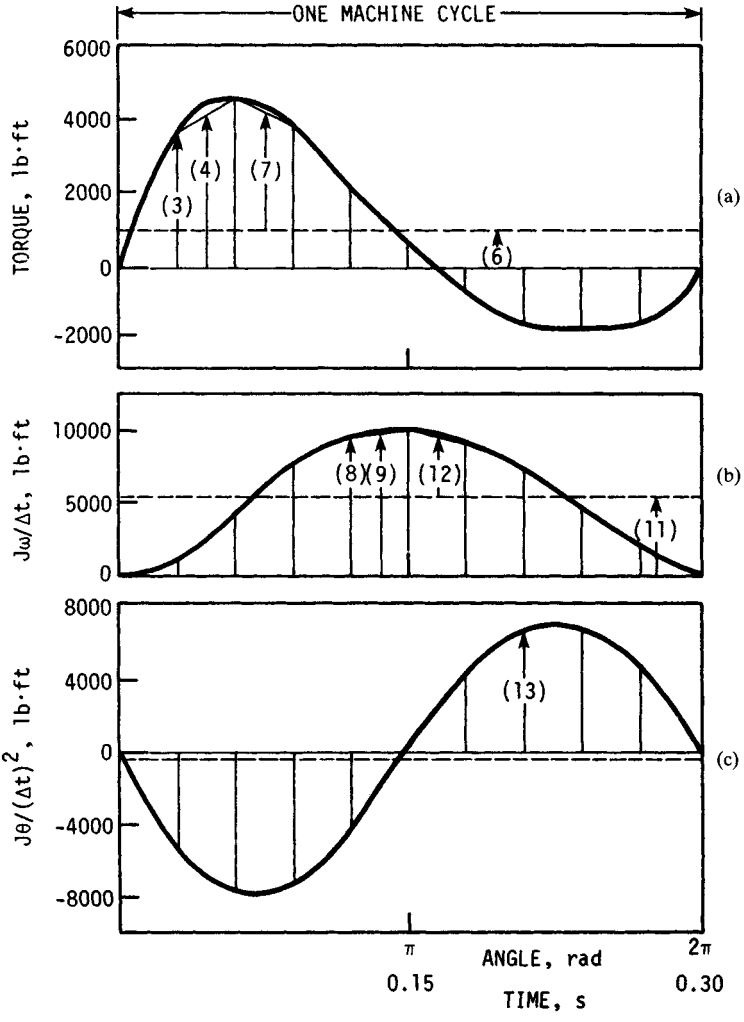

FIGURE 18.3 (*a*) Torque-angle or torque-time curve for Example 4. Dashed lines indicate average values, and the numbers in parentheses represent typical values found in Table 18.3. (*b*) Calculated rotational speed. (*c*) Calculated rotation angle.

18.2.5 Speed-Dependent Torques

The input and loading torques are in reality a function of angle, time, speed, acceleration, and other factors. In most cases, the assumption that they are functions of angle only is a good one. In some applications, however, different assumptions are necessary.

Figure 18.4 shows the torque-speed relationship for an induction motor. The curve can be approximated by a straight line $T_s = a\omega + b$ in the recommended oper-

TABLE 18.3 Numerical Integration for Example 4

j (1)†	t, s (2)	T, lb·ft (3)	Area, $[(3)_j + (3)_{j-1}]/2$, lb·ft (4)	Area − Avg. [(4) − (6)], lb·ft (7)	Sum Σ (7), lb·ft (8)	Area $[(8)_j + (8)_{j-1}]/2$, lb·ft (9)	Area − Avg. [(9) − (11)], lb·ft (12)	Sum Σ (12), lb·ft (13)
0	0	0	0	0	0	0	0	0
1	0.03	3670	1835‡	933	933	467	−4908	−4908
2	0.06	4628	4149	3247	4181	2557	−2818	−7725
3	0.09	3830	4229	3327	7508	5845	470	−7256
4	0.12	1931	2881	1979	9487	8498	3123	−4132
5	0.15	654	1293	391	9878	9683	4308	175
6	0.18	−734	−40	−942	8936	9407	4033	4208
7	0.21	−1628	−1181	−2083	6854	7895	2521	6729
8	0.24	−1739	−1684	−2585	4269	5561	187	6915
9	0.27	−1596	−1668	−2569	1700	2984	−2390	4525
10	0.30	0	−798	−1700	0	850	−4525	0
			(5) Sum 9016			(10) Sum 53 746		
			(6) Avg. 902			(11) Avg. 5375		

†See Example 4 and Fig. 18-3 for a description of each column.
‡The table entries were calculated to a higher precision and rounded.

ating range [18.7]. If the torque-angle curve is known for the loading torque T_a, the speed equation is

$$\omega^2(\theta) - \omega_0^2 = \frac{2}{J}\int_0^{\theta} [a\omega(\beta) + b - T_a(\beta)]\, d\beta \tag{18.22}$$

This equation is implicit in ω, and the initial value ω_0 is unknown. Dividing the angle for one cycle into intervals $\Delta\theta$ long and letting ω_j denote the speed at the end of j intervals, the trapezoidal rule gives

$$\omega_j^2 - \omega_0^2 = \frac{2}{J}\left(\frac{a(\omega_0 + 2\omega_1 + 2\omega_2 + \cdots + 2\omega_{j-1} + \omega_j)}{2} + jb - \frac{T_0 + 2T_1 + 2T_2 + \cdots + 2T_{j-1} + T_j}{2}\right)\Delta\theta \tag{18.23}$$

where T_0 through T_j are the values of T_a at the end of each interval. The unknowns in this equation are ω_j and ω_0. If a value for ω_0 is assumed, the quadratic equation gives

$$\omega_j = A_j + \sqrt{A_j^2 + B_j} \tag{18.24}$$

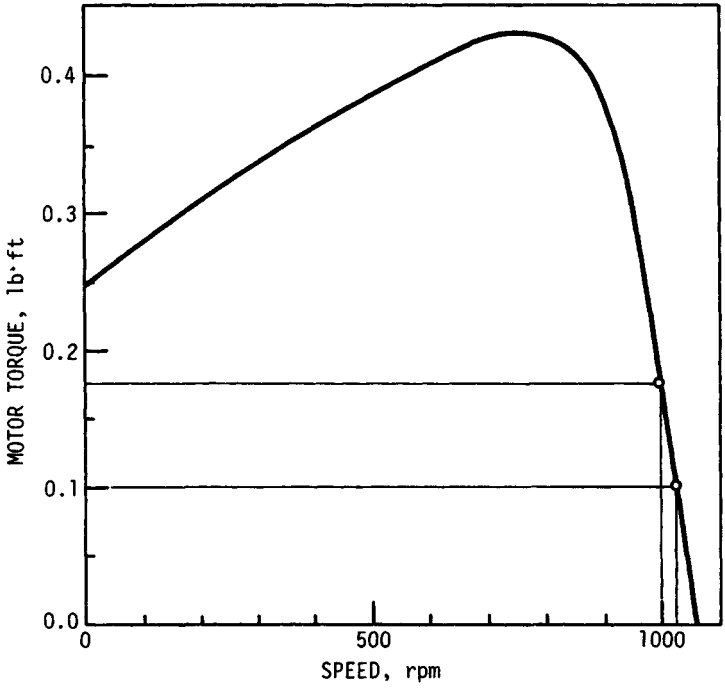

FIGURE 18.4 Torque-speed curve for the induction motor of Example 5. The curve can be approximated by a straight line near the recommended full-torque operating speed of 1000 rpm.

where

$$A_j = \frac{a\,\Delta\theta}{2J} \tag{18.25}$$

$$B_j = \omega_0^2 + \left[\frac{a}{2}(\omega_0 + 2\omega_1 + \cdots + 2\omega_{j-1}) + C_j\right]\frac{2\,\Delta\theta}{J} \tag{18.26}$$

and

$$C_j = jb - \frac{T_0 + 2T_1 + 2T_2 + \cdots + 2T_{j-1} + T_j}{2} \tag{18.27}$$

Equation (18.24) is solved successively for each j. The calculated value of ω at the end of the final interval will not in general equal the value that was originally assumed for ω_0. If the calculation is rerun with this final speed as the assumed value for ω_0, the numbers will be closer. After a few calculation cycles, the answers will converge.

Example 5. An induction motor provides 0.175 lb·ft of torque at the recommended full-load operating speed of 1000 rpm. The linear portion of the torque-speed curve also goes through the point of 0.102 lb·ft torque at 1025 rpm. Using the torque-angle curve for the load given in Fig. 18.5, find C_s if the load has the same 200-rpm speed as the flywheel and $J = 0.085$ lb·s^2·ft referred to the flywheel.

The motor has been chosen so that the average loading torque balances the motor torque at the recommended speed; since the speed of the motor is 1000/200 = 5 times the speed of the load, the average load should be approximately $T = 5(0.175) = 0.875$ lb·ft.

Referring the motor torques and speeds to the flywheel speed, the two points on the torque-speed curve become 0.175(5) = 0.875 lb·ft at 1000/5 = 200 rpm and 0.102(5) = 0.510 lb·ft at 1025/5 = 205 rpm. With 200 rpm = 2π(200)/60 = 20.944 rad/s

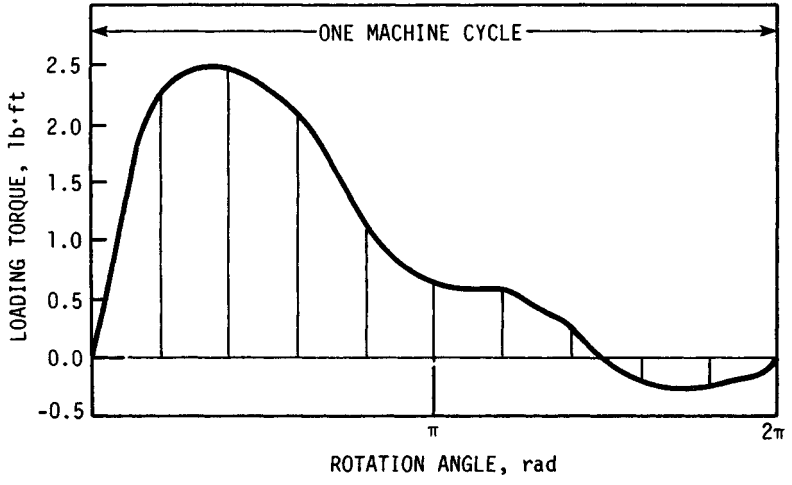

FIGURE 18.5 Torque-angle curve for the load in Example 5.

and 205 rpm = $2\pi(205)/60 = 21.468$ rad/s, the equation for the linear part of the torque-speed curve for the motor, referred to the flywheel, is given by the two-point formula

$$\frac{T_s - 0.875}{\omega - 20.944} = \frac{0.510 - 0.875}{21.468 - 20.944} \tag{18.28}$$

or

$$T_s = -0.697\omega + 15.46 \tag{18.29}$$

Therefore, $a = -0.697$ lb·s·ft/rad and $b = 15.46$ lb·ft.

For illustration purposes, the machine cycle will be divided into 10 intervals of $\pi/5$ rad each (see Fig. 18.5). For an accurate solution, the problem would be programmed on a computer with perhaps 50 intervals. The loading torque at the end of each interval is first tabulated as shown in column 3 in Table 18.4. The average torque in each interval, $0.5(T_{j-1} + T_j)$, is placed in column 4, and the cumulative sum of these numbers is placed in column 5. The values in column 5 thus represent the T summation in Eq. (18.27). In column 6 these values are subtracted from $jb = j(15.46)$ to form C_j. The values in columns 1 through 6 will not be changed in the iteration process.

For the first iteration, a value of $\omega_0 = 20.944$ rad/s is chosen as an initial guess of the speed at the start of the cycle. For $j = 1$, $\omega_{j-1} = \omega_0 = 20.944$ rad/s is placed in column 7. As column 7 is filled, column 8 will be formed as the summation $\omega_0 + 2\omega_1 + 2\omega_2 + \cdots + 2\omega_{j-1}$ required in Eq. (18.26). B_j is then evaluated from Eq. (18.26) using the values of a, C_j, ω_0, and $2\,\Delta\theta/J = 2(\pi/5)/0.085 = 14.784$ rad/(lb·s²·ft) and placed in column 9. With $A_j = -0.697(\pi/5)(0.5)/0.085 = -2.576$ rad/s, Eq. (18.24) can be evaluated to give ω_j. For $j = 1$, $\omega_1 = 20.87$ rad/s is thus placed in column 10. This value is then brought over to column 7 for $j = 2$ and the process is repeated until column 10 is filled. The last value in column 10, 21.59 rad/s, is the speed at the end of the cycle using the initial guess for ω_0. Then 21.59 rad/s is used as the ω_0 value for the second iteration, producing columns 11 through 14. This process is repeated until the final speed for the cycle equals the initial speed that was assumed. In this example this takes three iterations, giving the speed variation given in column 18.

The maximum and minimum speeds, from column 18, are 21.64 rad/s and 20.32 rad/s. From Eq. (18.1), C_s is then this range divided by the average:

$$C_s = \frac{\omega_{max} - \omega_{min}}{0.5(\omega_{max} + \omega_{min})} = \frac{21.64 - 20.32}{0.5(21.64 + 20.32)} = 0.063 \tag{18.30}$$

18.3 STRESS

18.3.1 Rim-Type: No Bending

If interaction with the spokes is ignored, the stress in a thin-rim flywheel is the uniform hoop stress:

$$\sigma = \frac{\rho r_a^2 \omega^2}{g} = \frac{\rho V^2}{g} \tag{18.31}$$

Since the stress is a function of velocity, the strength of flywheel materials can be given in terms of maximum rim velocity (see Sec. 18.5.1).

TABLE 18.4 Numerical Tabulation for Example 5

j	θ, rad	T	Avg.	Sum	C_j	ω_{j-1}	Sum†	B_j, (rad/s)^2	ω_j, rad/s	ω_{j-1}	Sum†	B_j, (rad/s)^2	ω_j, rad/s	ω_{j-1}	Sum†	B_j, (rad/s)^2	ω_j, rad/s
		lb·ft				rad/s				rad/s				rad/s			
(1)‡	(2)	(3)	(4)	(5)	(6)	(7)	(8)	(9)	(10)	(11)	(12)	(13)	(14)	(15)	(16)	(17)	(18)
0	0	0.00	0.000	0.000	....	....	....	....	20.94	....	....	....	21.59	....	....	....	21.64
1	$\pi/5$	2.22	1.110§	1.110	14.35	20.94	20.94	542.89	20.87	21.59	21.59	566.90	21.37	21.64	21.64	568.89	21.41
2	$2\pi/5$	2.43	2.325	3.435	27.49	20.87	62.68	522.07	20.42	21.37	64.33	540.86	20.82	21.41	64.47	542.42	20.86
3	$3\pi/5$	2.06	2.245	5.680	40.70	20.42	103.51	507.05	20.09	20.82	105.98	521.67	20.41	20.86	106.18	522.88	20.44
4	$4\pi/5$	1.08	1.570	7.250	54.59	20.09	143.69	505.40	20.05	20.41	146.79	516.71	20.30	20.44	147.05	517.66	20.32
5	π	0.62	0.850	8.100	69.20	20.05	183.79	514.77	20.26	20.30	187.40	523.52	20.45	20.32	187.69	524.25	20.46
6	$6\pi/5$	0.55	0.585	8.685	84.08	20.26	224.31	525.93	20.50	20.45	228.29	532.72	20.65	20.46	228.62	533.29	20.66
7	$7\pi/5$	0.23	0.390	9.075	99.15	20.50	265.31	537.47	20.75	20.65	269.59	542.75	20.86	20.66	269.94	543.19	20.87
8	$8\pi/5$	−0.20	0.015	9.090	114.59	20.75	306.81	551.99	21.06	20.86	311.31	556.11	21.15	20.87	311.69	556.45	21.15
9	$9\pi/5$	−0.26	−0.230	8.860	130.28	21.06	348.93	566.95	21.37	21.15	353.61	570.17	21.44	21.15	353.99	570.44	21.45
10	2π	0.00	−0.130	8.730	145.87	21.37	391.68	577.19	21.59	21.44	396.49	579.72	21.64	21.45	396.89	579.93	21.64
						$\omega_0 = 21.59$				$\omega_0 = 21.64$				$\omega_0 = 21.64$			

†$\omega_1 + 2\omega_2 + 2\omega_3 + \cdots + 2\omega_{j-1}$
‡See Example 5 for a description of each column.
§The table entries were calculated to a higher precision and rounded.

Example 6. An alloy of density 26.6 kN/m^3 has an allowable stress of 70 MPa. For a flywheel speed of 200 rad/s, what is the largest possible average radius, overlooking the additional stress caused by the spokes?

From Eq. (18.31),

$$V = \sqrt{\frac{g\sigma}{\rho}} = \sqrt{\frac{9.80(70)(1000)}{26.6}}$$

$$= 160.6 \text{ m/s} \tag{18.32}$$

and

$$r_a = \frac{V}{\omega} = \frac{160.6}{200} = 0.803 \text{ m} \tag{18.33}$$

18.3.2 Rim-Type: With Bending

If the effects of the spoke are taken into account, Timoshenko showed that the tensile stress in the thin rim (Fig. 18.6), including bending but neglecting the effect of the curvature on the bending stress and assuming spokes of constant cross-sectional area, can be calculated from beam theory using Castigliano's theorem [18.10], giving

$$\sigma = \frac{\rho r_a^2 \omega^2}{g}\left[1 - \frac{f_4}{3} + \frac{A r_a}{3 Z_r}\left(f_4 - \frac{1}{f_3 \alpha}\right)\right] \tag{18.34}$$

where

$$f_1 = \frac{1}{2\sin^2\alpha}\left(\frac{\sin 2\alpha}{4} + \frac{\alpha}{2}\right) \qquad f_2 = f_1 - \frac{1}{2\alpha} \tag{18.35}$$

$$f_3 = \frac{A r_a^2 f_2}{I} + f_1 + \frac{A}{A_s} \qquad f_4 = \frac{\cos\beta}{f_3 \sin\alpha} \tag{18.36}$$

and the section modulus of the rim Z_r is positive for the outer face of the rim and negative for the inner face. The stress in the spokes is given by

$$\sigma = \frac{\rho r_a^2 \omega^2}{6g}\left(3 + \frac{4A}{f_3 A_s} - \frac{3r^2}{r_a^2}\right) \tag{18.37}$$

In addition, there will be bending stresses in the spokes as power is exchanged with the flywheel. This torque might be determined by the maximum shaft torque, by the minimum braking time from full speed, or, if the flywheel also serves as a pulley, by the difference in belt force between the power and slack sides.

Depending on how thick the rim is, the spoke will behave as something between an end-loaded cantilever and a guided cantilever. For a thin rim, the maximum bending stress on the spokes will occur at the hub, assuming that they do not taper more than the usual 10 to 25 percent. This bending stress is

$$\sigma = \frac{T(r_a - r_h)}{Z_s N_s r_a} \tag{18.38}$$

If the flywheel serves as a pulley, the torque is not equally distributed to the spokes; the value for N_s should be halved in this case. For a flywheel with a large rim

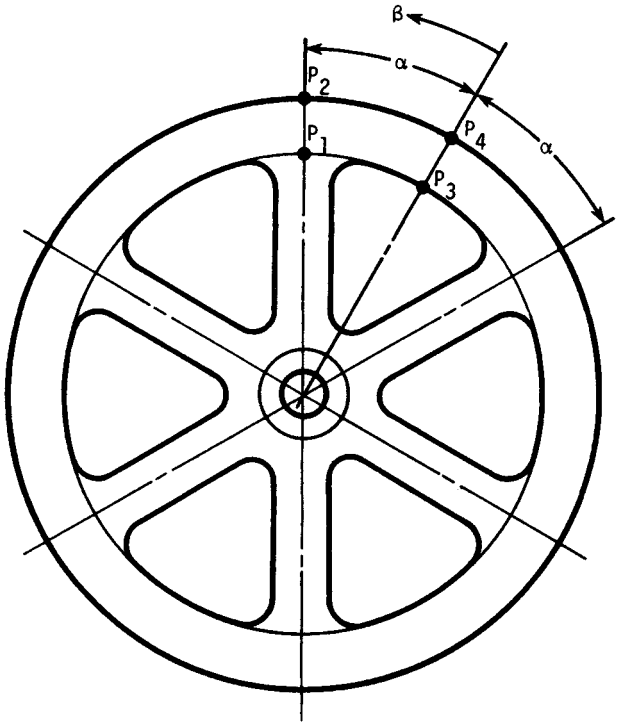

FIGURE 18.6 Rim-type flywheel. The angular position β is measured from the center line bisecting the adjacent spoke locations. Points P_1 through P_4 correspond to the values given in Table 18.5.

section in comparison to the spokes, the spokes act as guided cantilevers and have a maximum bending stress that is half the value given by Eq. (18.38).

Example 7. A cast-iron flywheel with a rectangular rim 5 in thick and 11 in wide has an average radius of 48 in. If the hub has a 5.2-in radius and each of the 8 spokes has an area of 11 in^2, what are the maximum stresses at a speed of 400 rpm? The maximum torque possible is 4000 lb·ft at full speed.

The area $A = (5)(11) = 55$ in^2, $\omega = 2\pi(400)/60 = 41.9$ rad/s, $I = 11(5)^3/12 = 114.6$ in^4, and $Z_r = 11(5)^2/6 = 45.8$ in^3. The angle α is 22.5 degrees, or $\pi/8$, and the maximum rim stress occurs at the inner surface of the rim with $\beta = \pi/8$. From Eqs. (18.34) through (18.36), using a density of 0.283 lb/in^3,

$$f_1 = \frac{1}{2\sin^2(\pi/8)}\left[\frac{\sin(\pi/4)}{4} + \frac{\pi/8}{2}\right] = 1.274 \tag{18.39}$$

$$f_2 = 1.274 - \frac{1}{\pi/4} = 7.600 \times 10^{-4} \tag{18.40}$$

$$f_3 = \frac{55(48)^2 7.600 \times 10^{-4}}{114.6} + 1.274 + \frac{55}{11} = 7.11 \tag{18.41}$$

$$f_4 = \frac{\cos(\pi/8)}{7.11 \sin(\pi/8)} = 0.340 \tag{18.42}$$

$$\sigma = \frac{0.283(48)^2(41.9)^2}{32.2(12)}\left[1 - \frac{0.340}{3} + \frac{55(48)}{3(-45.8)}\left(0.340 - \frac{1}{7.11\pi/8}\right)\right] = 3660 \text{ psi} \tag{18.43}$$

Table 18.5 shows the values for points P_1, P_2, P_3, and P_4, giving additional digits for checking computer programs. Although the stress formulation was based on a spoke of length r_a, the maximum tension stress in the spoke is found for the hub radius, 5.2 in. From Eq. (18.37),

$$\sigma = \frac{0.283(48)^2(41.9)^2}{6(32.2)(12)}\left[3 + \frac{4(55)}{7.11(11)} - \frac{3(5.2)^2}{(48)^2}\right] = 2850 \text{ psi} \tag{18.44}$$

If the spokes are of standard design, an elliptical cross section twice as long in the direction of motion as in the axial direction, the dimensions for an 11-in^2 spoke would be $\sqrt{2(11)/\pi} = 2.65$ in by 5.29 in. The section modulus is then $Z_s = \pi(2.65)(5.29)^2/32 = 7.28$ in^3, and the bending stress in the spokes, from Eq. (18.38), would be

$$\sigma = \frac{4000(48 - 5.2)}{7.28(8)(48)} = 61 \text{ psi} \tag{18.45}$$

The combined stress for the spoke is then $\sigma = 2850 + 61 = 2910$ psi.

18.3.3 Thin Disk

If a thin disk has a large radius in comparison to its thickness, the stress can be assumed constant across the thickness. Defining the stress function F as

$$F = rz\sigma_r \tag{18.46}$$

the stress equation for a thin disk of variable thickness $z(r)$ is

$$r^2\frac{d^2F}{dr^2} + r\frac{dF}{dr} - F + (3+\nu)\frac{\rho\omega^2 r^3 z}{g} - \frac{r}{z}\frac{dz}{dr}\left(r\frac{dF}{dr} - \nu F\right) = 0 \tag{18.47}$$

and

$$\sigma_t = \frac{1}{z}\frac{dF}{dr} + \rho\omega^2 r^2 \tag{18.48}$$

TABLE 18.5 Rim Stress for Example 7

Term	P_1	P_2	P_3	P_4
Z_r, in^3	−45.833 3	45.844 3	−45.833 3	45.833 3
β	$\pi/8$	$\pi/8$	0	0
f_1	1.273 93	1.273 93	1.273 93	1.273 93
f_2 ($\times 10^{-4}$)	6.932 02	6.932 02	6.932 02	6.932 02
f_3	7.040 56	7.040 56	7.040 56	7.040 56
f_4	0.342 901	0.342 901	0.371 153	0.371 153
σ, psi	3690.32	1554.43	2056.37	3132.62

The boundary conditions for the center or inner radius and the outer radius are both $F = 0$. If there is a central bore, a finite value for r_i is used in the formulation, and for an infinitesimal hole, the limit is taken later. At the center of the solid disk, $\sigma_r = \sigma_t$. The inertia for a disk is given by

$$J = \int_{r_i}^{r_o} \frac{2\pi\rho r^3 z}{g}\, dr \tag{18.49}$$

Equations (18.46) through (18.48) can be solved explicitly for the uniform and hyperbolic profiles [18.4]. For the general case, using a difference approximation for dz/dr and F leads to a tractable banded set of linear simultaneous equations. Divide the radius into equal intervals of length Δr. Determine the z derivative for each point using

$$z'_j = \frac{z_{j+1} - z_{j-1}}{2\,\Delta r} \tag{18.50}$$

except at the two boundaries, where, for the same accuracy,

$$z'_j = \frac{2z_{j+3} - 9z_{j+2} + 18z_{j+1} - 11z_j}{6\,\Delta r} \tag{18.51}$$

at the center or inner radius and

$$z'_j = \frac{11z_j - 18z_{j-1} + 9z_{j-2} - 2z_{j-3}}{6\,\Delta r} \tag{18.52}$$

at the outer radius. The stress equation then becomes the set of equations

$$A_j F_{j-1} + B_j F_j + C_j F_{j+1} = D_j \tag{18.53}$$

where

$$A_j = \frac{r_j}{\Delta r}\left(\frac{r_j}{\Delta r} - \frac{1}{2} + \frac{r_j}{2}\frac{z'_j}{z_j}\right) \tag{18.54}$$

$$B_j = -2\left(\frac{r_j}{\Delta r}\right)^2 + \nu r_j\left(\frac{z'_j}{z_j}\right) - 1 \tag{18.55}$$

$$C_j = \frac{r_j}{\Delta r}\left(\frac{r_j}{\Delta r} + \frac{1}{2} - \frac{r_j}{2}\frac{z'_j}{z_j}\right) \tag{18.56}$$

$$D_j = -(3+\nu)\frac{r_j^3 z_j \rho\omega^2}{g} \tag{18.57}$$

At the two boundary points the equation is identically satisfied, leaving $(r_o - r_i)/\Delta r - 1$ equations. For the inner equation, $A_j = 0$, and for the outer equation, $C_j = 0$. The simultaneous equations are solved for F_j, and the stresses are found from Eqs. (18.46) and (18.48). See the user's guide for your computer for a convenient method of solving linear simultaneous equations.

18.3.4 Disk of Constant Thickness

The solutions for a disk of uniform thickness are simplified if a constant is defined as

$$\sigma_0 = \frac{\rho r_o^2 \omega^2 (3+\nu)}{8g} \tag{18.58}$$

For a constant-thickness disk without a central hole, the radial and tangential stresses are then given by

$$\sigma_r = \sigma_0\left(1 - \frac{r^2}{r_o^2}\right) \tag{18.59}$$

$$\sigma_t = \sigma_0\left(1 - \frac{1+3\nu}{3+\nu}\frac{r^2}{r_o^2}\right) \tag{18.60}$$

and the maximum stress, at $r = 0$, is

$$\sigma_{r,\max} = \sigma_{t,\max} = \sigma_0 \tag{18.61}$$

For a disk with a central hole, the stresses are given by

$$\sigma_r = \sigma_0\left(1 - \frac{r^2}{r_o^2} + \frac{r_i^2}{r_o^2} - \frac{r_i^2}{r^2}\right) \tag{18.62}$$

$$\sigma_t = \sigma_0\left(1 - \frac{1+3\nu}{3+\nu}\frac{r^2}{r_o^2} + \frac{r_i^2}{r_o^2} + \frac{r_i^2}{r^2}\right) \tag{18.63}$$

The maximum radial stress, at $r = \sqrt{r_o r_i}$, is

$$\sigma_{r,\max} = \sigma_0\left(1 - \frac{r_i}{r_o}\right)^2 \tag{18.64}$$

and the maximum tangential stress, at $r = r_i$, is

$$\sigma_{t,\max} = \sigma_0\left(2 + \frac{2-2\nu}{3+\nu}\frac{r_i^2}{r_o^2}\right) \tag{18.65}$$

The inertia is

$$J = \frac{\pi\rho z}{2g}(r_o^4 - r_i^4) \tag{18.66}$$

Example 8. A steel disk of uniform thickness and outer radius 0.6 m rotates at 30 rad/s. Find the maximum stress in the disk if it has an integral shaft, neglecting stress rises due to the geometry change at the shaft. What is the maximum disk stress if the disk is bored for a shaft of 0.025-m radius?

The stress is independent of thickness. From Eqs. (18.58) and (18.61) with $\rho = 76.5$ kN/m^3 and $\nu = 0.3$,

$$\sigma_{r,\max} = \sigma_{t,\max} = \sigma_0$$

$$= \frac{76.5(0.6)^2(30)^2(3+0.3)}{8(9.80)(1000)} = 1.043 \text{ MPa} \tag{18.67}$$

For the bored disk, the maximum radial stress occurs at $r = \sqrt{0.6(0.025)} = 0.122$ m. From Eq. (18.64),

$$\sigma_{r,\max} = 1.043\left(1 - \frac{0.025}{0.6}\right)^2 = 0.958 \text{ MPa} \tag{18.68}$$

The maximum tangential stress occurs at the hub. From Eq. (18.65),

$$\sigma_{t,\max} = 1.043\left[2 + \frac{2-2(0.3)}{3+0.3}\frac{(0.025)^2}{(0.6)^2}\right]$$

$$= 2.09 \text{ MPa} \tag{18.69}$$

18.4 FLYWHEELS FOR ENERGY STORAGE

The flywheel can be used as an energy reservoir, with energy being supplied at a slow constant rate or when it is available and being withdrawn when desired. A flywheel might, for example, be used to give good acceleration to an automobile that is underpowered by present standards. Regenerative breaking, power storage for peak-demand periods, and mechanical replacements for battery banks are all potential uses for the flywheel. The high charging and discharging rates of a flywheel system give it an advantage over other portable sources of power, such as batteries.

Although the concepts developed in the previous sections are still true for energy-storage flywheels, the purpose is now to store as much kinetic energy, $0.5J\omega^2$, as possible. In most applications, the flywheel speed does not vary over 50 percent, so that only about 75 percent of this total energy is actually recoverable. The design of the ordinary flywheel is usually dictated by the allowable diameter, governed by the machine size, and the maximum speed, governed by the practicalities of a speed-increasing drive and higher bearing speeds. These constraints can result in a low peripheral speed, causing the economics to favor a rim-type flywheel design. The economics change with the energy-storage flywheel, since (1) larger values of total stored energy are usually involved, requiring heavier flywheels or more energy per unit weight of flywheel, (2) the weight of a heavy flywheel and the correspondingly heavy bearings and other components may be unacceptable, especially in mobile applications, and (3) the design constraints imposed in a machine where the flywheel limits the speed variation can be relaxed when the flywheel is the main component, encouraging optimization. Depending on the application, the energy per dollar, energy per weight, or energy per swept volume is usually maximized [18.1].

18.4.1 Isotropic and Anisotropic Designs

The stress equations for the thin disk given in Sec. 18.3.3 can be solved with $\omega_r = \omega_t$ to give the shape for a fully stressed thin isotropic disk with no central bore:

$$z = z_0 \exp\left(-\frac{\rho\omega^2 r^2}{2gS_y}\right) \tag{18.70}$$

where S_y = allowable strength, for example, the yield strength of the material. Define the energy stored per unit weight as

$$R = F_s\frac{S_y}{\rho} \tag{18.71}$$

where F_s is a dimensionless factor that depends only on the shape of the flywheel. Using Eqs. (18.46) through (18.49), it turns out that the efficiency or geometric shape

factor $F_s = 1.0$ for the fully stressed profile. As Eq. (18.70) indicates, this profile has an infinite outer radius; truncating the profile reduces F_s substantially. Modifying the profile can improve the efficiency, increasing F_s to 0.97 (see Table 18.6), but that is the limit for a homogeneous isotropic design. To avoid this basic limitation and to take advantage of the higher strength-to-weight and stiffness-to-weight ratio of composite materials, recent efforts have concentrated on anisotropic designs ([18.1], [18.8]). Figure 18.7 describes a few of the many designs that are being developed.

18.4.2 Special Considerations

Energy-storage flywheels have special problems which are related to their high speed, flexibility, and anisotropy. The increased operational speed requires high-speed power transmission and bearings as well as special attention to drag forces and the critical vibration speeds of the torsional system. A continuously variable transmission and operation in a vacuum are usually required. Forward whirling is a potentially serious problem that may limit the operating range or require external damping [18.3]. The flexibility can cause flywheel vibration modes with frequencies in the operating range and can also cause significant imbalance to occur as the flywheel deforms with speed. Anisotropy can cause failure in the weak direction (matrix failure or delamination) before the full strength in the strong direction is utilized.

18.5 STRENGTH AND SAFETY

18.5.1 Materials

Neglecting gravity and other secondary loads, the stresses in a flywheel will be proportional to $V^2 = (r_o\omega)^2$. Two flywheels of the same design but of different size will therefore have the same rim stress when their rim velocities are equal. Also, since the stress is proportional to V^2, a 10 percent increase in rotational speed will cause a 21 percent increase in stress. Although the strengths of flywheel materials are sometimes given in terms of their maximum rim velocities, these strengths include generous factors of safety to account for all the possible variations in the material properties, design details, and methods of manufacture. A rational approach would

TABLE 18.6 Shape Factor for Several Isotropic Flywheel Shapes

Shape	F_s
Fully stressed, infinite radius	1.00
Optimum, finite radius	0.97
Exponential or truncated conical (approximate)	0.8
Uniform thickness	0.61
Thin-rim type	0.50
Bar	0.33
Uniform thickness, central bore	0.31

SOURCE: From Gilbert et al. [18.5], by permission.

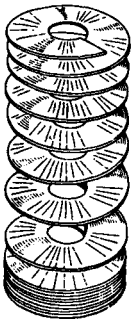

(a)

(b)

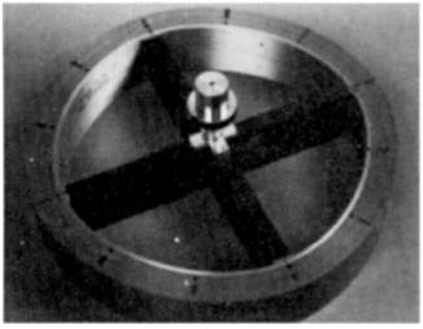

(c)

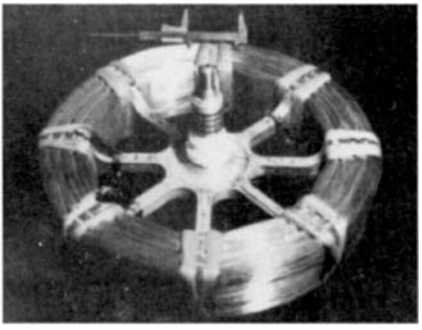

(d)

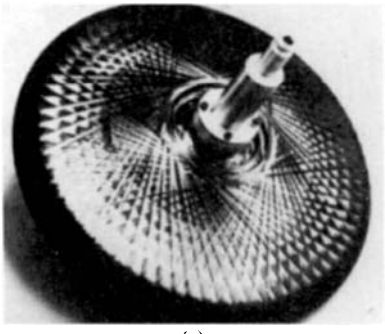

(e)

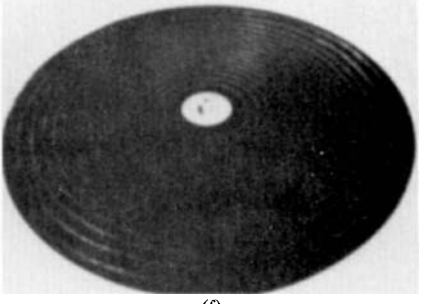

(f)

FIGURE 18.7 Energy-storage flywheel designs. (*a*) Flywheel of helically woven fabric with variable properties in the radial and circumferential directions (*exploded view*) (*Avco Systems Division*); (*b*) filament-wound graphite/epoxy rim with laminated S2-glass/epoxy disk (*General Electric Company*); (*c*) subcircular multilayer rim of S-glass and Kevlar, with graphite/epoxy spokes (*Garrett AiResearch Corporation*); (*d*) bare-filament Kevlar rim with aluminum hub (*Istituto della Motorizzazione, Torino, Italy, built by Industrie Pirelli S.p.A. and sponsored by the Italian National Research Council*); (*e*) graphite/epoxy and steel-filament/epoxy rim with a woven graphite/epoxy overwrap (*MAN Advanced Technology, Munich, Germany*); (*f*) variable-thickness graphite/epoxy laminated disk (*Lawrence Livermore National Laboratory*).

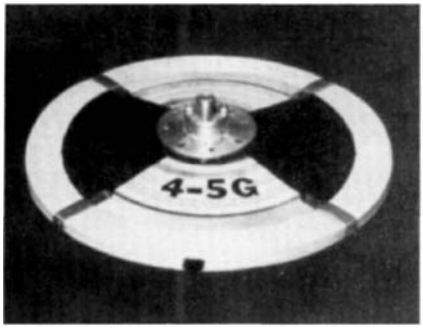

(g)

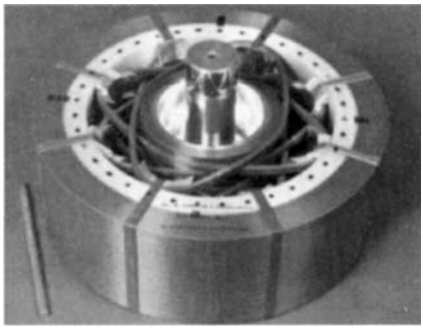

(h)

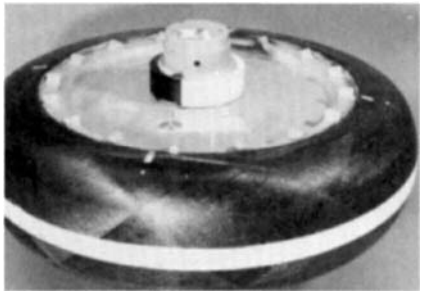

(i)

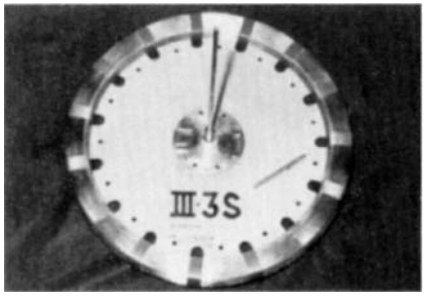

(j)

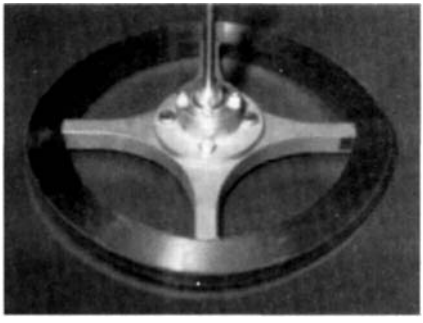

(k)

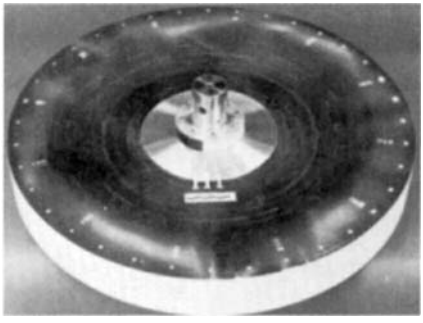

(l)

FIGURE 18.7 *(Continued)* Energy-storage flywheel designs. (*g*) bare-filament high-strength steel-wire rim, as used in steel-belted radial tires, with fiberglass hub (*The Johns Hopkins University Applied Physics Laboratory*); (*h*) multilayer rim of S-glass and Kevlar, with catenary tension-balanced spokes (*William M. Brobeck and Associates*); (*i*) graphite/epoxy-wound rim with overwrap over an aluminum liner with two contoured-aluminum hubs (*Rockwell International/Rocketdyne Division*); (*j*) vinyl-coated S-glass rim with Russian birch hub (*The Johns Hopkins University Applied Physics Laboratory*); (*k*) Metglas (amorphous steel) ribbon rim with aluminum spokes (*The Johns Hopkins University Applied Physics Laboratory*); (*l*) contoured graphite/epoxy filament-wound disk (*Hercules Aerospace*). (Kevlar is a registered trademark of E. I. du Pont de Nemours and Company, Inc.; Metglas is a registered trademark of The Allied Corporation.) (*Photographs assembled with the assistance of W. Wilkinson, The Johns Hopkins University Applied Physics Laboratory, and S. Kulkarni, The Lawrence Livermore National Laboratory; by permission.*)

be to assign risk factors to each unknown in the specific flywheel design and multiply the resulting factors of safety or, if sufficient data are available, to use a probabilistic or statistical approach [18.6] (see also Chap. 2).

Cast iron has often been chosen as a flywheel material on the basis of cost per pound. However, this criterion is valid only if the design constraints on radius and speed dictate a low rim stress. Otherwise the higher strength-to-weight ratio of other materials may make them less expensive. With any cast flywheel there is the possibility of brittleness, of blowholes, and of other casting flaws; shrinkage stresses in the casting must also be controlled. To reduce shrinkage stresses, one-piece flywheels larger than a few feet in diameter are often cast with a split hub, i.e., with each separate arc of the hub allowed to move with the attached spokes. After cooling, the hub is then bolted together using spacer plates.

The rim is sometimes cast separately from the spokes, and special care must be taken to design an efficient joint between the two. On flywheels larger than 10 ft in diameter, the rim is sometimes fabricated in two or more sections, usually for transportation reasons. The joint efficiency in these cases can be as low as 30 percent, and so extreme care should be taken in designing the joint. The more efficient designs rely on bow tie or ring shrink-fit connectors placed at the spoke locations. A more advanced study should be made unless the calculated stresses are markedly low; a photoelastic or finite-element model [18.9] might be constructed, for example.

Cast steel is stronger than cast iron and is widely used. Flame-cut steel-plate flywheels are relatively inexpensive to manufacture, and their simplicity may make up for their inefficient shape. Flywheels welded from steel plate are inherently stronger than cast flywheels as long as proper care is taken to control flaws and residual weld stresses.

18.5.2 Safety

If the designer can reduce the uncertainty in any of the design unknowns, the necessary factor of safety will be less and a lighter flywheel will result. Design unknowns include (1) material properties, (2) analysis error, (3) loading, and (4) installation. The material properties of the finished flywheel may vary due to welds, porous casting, or lamination flaws. The analysis may have been an elementary beam calculation or a detailed finite-element/fatigue/fracture mechanics study. The input and output loads and speeds may be estimated, calculated, or measured values. The skill or care used in installation may be unknown or well controlled. Improvement in any of these areas will give a better design.

Another way to reduce the necessary factor of safety is through testing. Both destructive and nondestructive tests of the material are excellent tools in answering questions about material properties and fabrication technique. The spin test, of course, is the primary proof of the material, fabrication, and design. Although it will not ordinarily answer questions of fatigue or cycled loads, a destructive spin test gives the best indication of the true safety margin. Long-term cyclic life tests are very helpful if a realistic load cycle can be devised.

A third way to reduce the necessary factor of safety is to reduce the physical and financial harm that would be caused by a flywheel failure. No matter what material is used, any flywheel will break if it is rotated fast enough. If this failure can be controlled in some way, the design speed of the flywheel can be closer to the failure speed without undue risk. Standard steel rim-type and disk flywheels usually burst into three to six pieces at failure; each piece travels with quite a bit of kinetic energy. One method to control failure is therefore to force a breakup into smaller pieces;

many composite flywheels shred, for example. Another method used with the energy-storage flywheel relies on centrifugal force to separate the outer circular sections of the flywheel from the spokes or inner hub section before the material begins to fail. If a benign failure mode cannot be introduced into the design, a heavier containment enclosure could serve the same purpose, lessening the consequence of a flywheel failure.

REFERENCES

18.1 *1980 Flywheel Technology Symposium,* October 1980, Scottsdale, Arizona, University of California Lawrence Livermore National Laboratory, Livermore, Calif., NTIS CONF-801022.

18.2 Rowland S. Benson and N. D. Whitehouse, *Internal Combustion Engines,* Pergamon, New York, 1979.

18.3 C. W. Bert and G. Ramunujam, "Design Guide for Composite-Material Flywheels: Rotor Dynamic Considerations, Part I," University of Oklahoma, Norman, Okla., September 1981, UCRL-15420.

18.4 J. P. Den Hartog, *Advanced Strength of Materials,* McGraw-Hill, New York, 1952.

18.5 R. R. Gilbert, et al., "Flywheel Feasibility Study and Demonstration," Lockheed Missiles and Space Company, Sunnyvale, Calif., April 1971, NTIS PB-200143.

18.6 Edward B. Haugen, *Probabilistic Approaches to Design,* John Wiley & Sons, New York, 1968.

18.7 Charles R. Mischke, *Elements of Mechanical Analysis,* Addison-Wesley, Reading, Mass., 1963.

18.8 R. P. Nimmer, K. Torossian, and W. W. Wilkening, "Laminated Composite Disk Flywheel Development," General Electric Company, Schenectady, N.Y., UCRL-15383.

18.9 M. Saraph, A. Midha, and J. C. Wambold, "Automated Stress Analysis of Mechanical Sheaves and Pulleys," *Computers in Mechanical Engineering,* pp. 34–42, October 1982.

18.10 Joseph E. Shigley and Charles R. Mischke, *Mechanical Engineering Design,* 5th ed., McGraw-Hill, New York, 1989.

18.11 Joseph Edward Shigley and John Joseph Uicker, Jr., *Theory of Machines and Mechanisms,* 2d ed. McGraw-Hill, New York, 1995.